33rd Annual International Conference of the IEEE EMBS
Boston, Massachusetts USA, August 30 - September 3, 2011

# Geographic Atrophy Segmentation in Infrared and Autofluorescent Retina Images using Supervised Learning

K Devisetti, *Member, IEEE,* T. P. Karnowski, *Member, IEEE,* L. Giancardo, *Member, IEEE,* Y. Li, Ph.D., *Member, IEEE,* E. Chaum, M.D., Ph.D., *Member, IEEE*

*Abstract*— **Geographic Atrophy (GA) of the retinal pigment epithelium (RPE) is an advanced form of atrophic age-related macular degeneration (AMD) and is responsible for about 20% of AMD-related legal blindness in the United States. Two different imaging modalities for retinas, infrared imaging and autofluorescence imaging, serve as interesting complimentary technologies for highlighting GA. In this work we explore the use of neural network classifiers in performing segmentation of GA in registered infrared (IR) and autofluorescence (AF) images. Our segmentation achieved a performance level of 82.5% sensitivity and 92.9% specificity on a per-pixel basis using hold-one-out validation testing. The algorithm, feature extraction, data set and experimental results are discussed and shown.**

## I. INTRODUCTION

Automated retina image processing and analysis has been become a leading topic of research in the medical imaging community in recent years, in part due to the growing need for affordable, scalable screening of diabetics for eye disease [1]. This work is also benefitting the automated processing of other important retinal diseases such as age-related macular degeneration (AMD). AMD, the leading cause of blindness in patients over the age of 65 in the industrialized world, is a degenerative disease of the retina of multifactorial etiology that preferentially affects central macular vision. Initial stages of AMD are characterized by sub-retinal deposits called drusen and progressive degeneration and atrophy of the retinal pigment epithelial layer of cells beneath the retina. Advanced AMD is characterized by areas of nummular geographic atrophy (GA, the *dry* form) or development of choroidal neovascularization (CNV, the wet form), abnormal subretinal vessels. Areas of GA and associated RPE cell death lead to degeneration of the overlying neurosensory retina and the underlying choriocapillaris [2,3]. Geographic atrophy is typically characterized by round lesions with sharply demarcated margins and changes in color and pigmentation relative to the surrounding areas of RPE. These changes in deep tissue pigmentation are documented in clinical practice using spectral-domain OCT confocal scanning laser ophthalmoscopy (cSLO). These technologies enable routine visualization of changes in the RPE manifesting as atrophy and loss of autofluorescence. The result is high contrast images that are more clearly defined than those produced by conventional fundus cameras. Multi-modality imaging provides image data which combine to offer clinicians a more comprehensive diagnostic assessment of AMD.

The objective of this paper is to report on a supervised learning algorithm implementation for retinal image segmentation using two imaging modalities, infrared (IR) and autofluorescent (AF) images of the same retina. We discuss the imaging modalities and their unique features, followed by a summary of our registration and segmentation approach. We then discuss our experimental approach and conclude with observations on results and recommendations for future research.

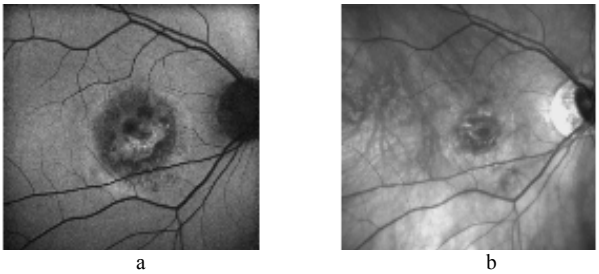

a b

Fig 1. Registered AF image (left) and IR image (right) of an area of geographic atrophy. Note that the extent of RPE disease is more easily seen as a dark lesion in the AF image. The optic nerve is at the right.

## II. BACKGROUND

Two useful modalities for investigating degenerative changes in the pigmented RPE are IR and AF images described above. Both IR and AF images are acquired using a laser beam which is periodically deflected by means of oscillating mirrors to sequentially scan a 2D retina. The intensity of the reflected light or the emitted fluorescent light at each point is measure with a light sensitive detector. The wavelength of laser used for IR images and AF images are 820 nm and 488 nm respectively. The AF images depict the

Manuscript received April 15, 2011. This work supported in part by the National Eye Institute of the National Institutes of Health (R01 EY017065), Research to Prevent Blindness, New York, NY, the Plough Foundation, Memphis TN. This paper was prepared by University of Tennessee Health Science Center, Memphis, TN-38163 and OAK RIDGE NATIONAL LABORATORY, Oak Ridge, TN, USA, 37831-6285, operated by UT-BATTELLE, LLC for the US DEPARTMENT OF ENERGY under contract DE-AC05-00OR22725.

K. Devisetti, E. Chaum and Y. Li are with the University of Tennessee Health Science Center, 930 Madison Avenue, Suite 731, Memphis TN 38163. Dr. Chaum is an RPB Senior Scientist.

T.P. Karnowski and L. Giancardo are with the Oak Ridge National Laboratory, Oak Ridge, TN 37831 USA.

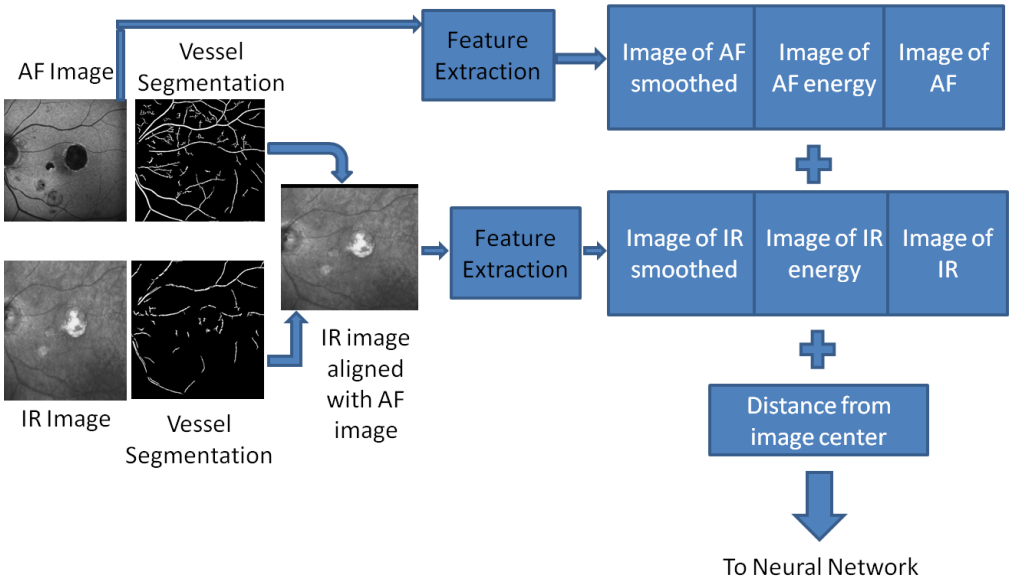


Fig 2. Flowchart indicating the sequence of operations performed during our segmentation using supervised learning. The AF and IR images are registered using reference points (seen in their vessel segmentation images). Different features like the image itself, smoothed image, energy of the image and distance from center of the image are extracted and given as inputs to a Neural Network algorithm.

emission of fluorescence from the RPE (the tissue layer beneath the retina). GA is characterized by the absence of signal (black blob) in the RPE. The infrared images on the other hand are obtained by the light collected from the reflection of the infrared light focused on the eye. Here, since the RPE is absent, the sclera (a white layer beneath the RPE and choroidal vessels) is seen. So, GA appears as dark region in AF images and light region in IR images.

## III. TECHNICAL APPROACH

In this section we discuss the fusion approach for the IR and AF images, focusing on issues of registration and feature extraction. An overview of our processing methodology is shown in Figure 2.

### *A. Physiological Feature Segmentation*

There are two key physiological features of interest in these images which were removed from processing. The first is the optic nerve (ON), as seen on the right side of Figure 1. Although there are approaches in the literature for optic nerve segmentation (such as [4]), we did not pursue these algorithms in this work and simply manually segmented the optic nerve region. The second, the vessel segmentation, also benefits from an extensive body of literature (such as [10]). We used the method of Klein [5] which performs morphological reconstruction operations focusing on multiple angles to emphasize the typically long, narrow vessel structures. We found this method to work well for this data in performing image registration and in masking out vessel pixels for supervised learning.

### *B. Image Registration*

The acquisition of IR and AF images are done sequentially and therefore the images are not generally registered. There are some challenges associated with registering the images since different features are highlighted in each modality. However, the vascular structure has the same image intensity and thus serves as a feature-rich structure with good potential for registration. There are existing algorithms to register retinal images described in the literature (such as [6-8]). For our image set, we used a brute-force method based on the vessel segmentation of both images. The AF image is considered as the base/reference image and the IR image is translated in space to align itself with the AF image. Normalized correlation [9] is used as a parameter to measure how well the images are registered. The IR image is then rotated across multiple rotation angles ranging from -12º to +12º in steps of 0.1º where 0º corresponds to the original, un-rotated image. Normalized correlation is re-evaluated till optimum registration is achieved. We did not adjust for scale in our image set, but we would have pursued a similar strategy of brute-force search had the situation warranted this. Also, all images from each modality were taken with the same instrument, so we did not attempt to use deformable registration to compensate for image acquisition differences.

### *C. Feature Extraction*

A supervised learning approach was taken where pixels which indicated geographic atrophy were designated by an ophthalmologist (as described in the next section). In order to adequately describe each pixel, a set of 7 features were extracted from the registered image pairs. These features are as follows: intensity of the IR image; intensity of the AF image; smoothed IR and AF intensities; local energy of the IR and AF images, computed in a neighborhood area of 20 pixels around pixel (x,y) as

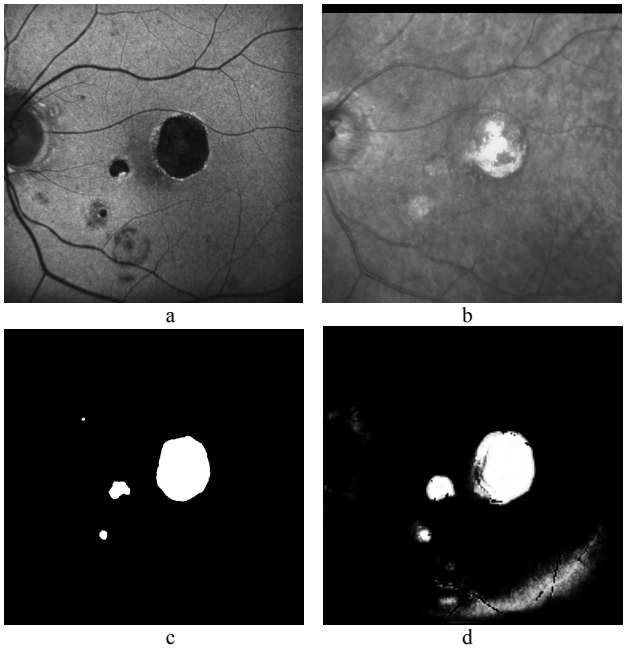


Fig. 3. GA segmentation example. (a) Original AF image (b) Registered IR image (c) Ground-truth (d) Segmentation result

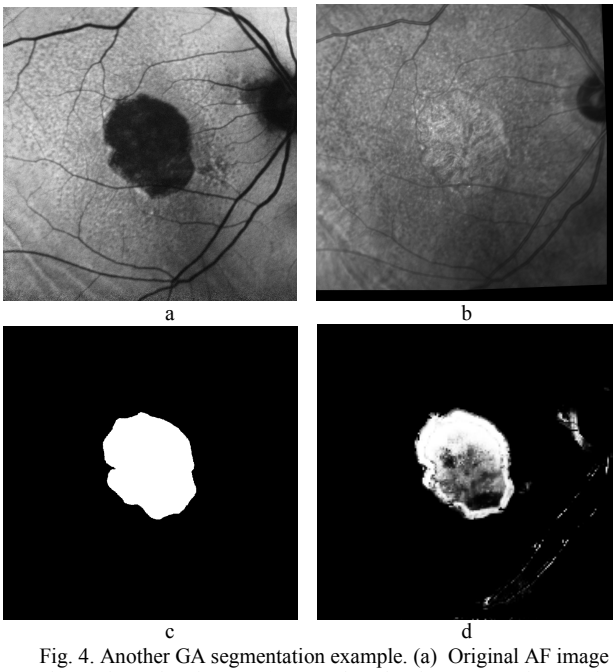


Fig. 4. Another GA segmentation example. (a) Original AF image (b) Registered IR image (c) Ground-truth (d) Segmentation result

$$E(x,y) = \sqrt{\sum\sum (I(x,y) - \hat{I}(x,y))^2} \ ,$$

where I(x,y) is the image intensity at pixel (x,y) and $\hat{I}(x,y)$ is the average intensity of the image in the same neighborhood. An additional feature was created which is the distance from the center of the image. In all cases, pixels which were located within the optic nerve region and the segmented vessel region were not included in the calculations of neighborhood operations, or were omitted altogether in the case of the non-neighborhood operations.

## IV. EXPERIMENTS

### A. Data Set

Deidentified AF and IR retinal images were obtained from the clinical practice at the University of Tennessee Health Science Center Hamilton Eye Institute, Memphis, TN in an IRB approved exempt study using the Heidelberg Spectralis HRA+OCT. The IR image and the AF image are acquired at same image size, 1536×1536 pixels, and at 30º field of view (FOV) to ensure easy comparison and analysis. Most of the images were acquired after the patient's pupil was dilated with eye drops. The AF and IR images are acquired one after the other which causes them to be shifted in space because of patient motion in between the image acquisitions. Moreover, the flashes of light that shines on the patient's eyes can cause the patient to move and hence cause additional spatial shift. The AF and IR images were extracted to TIF format from their original DICOM format and were sized 1536 x 1536 pixels, with roughly 3.73 pixels/mm resolution. Images were ground-truthed by a practicing ophthalmologist (E. Chaum) who delineated the GA on the AF images using an interactive GUI developed by us.

### B. Automated Processing Experiments

For the image registration, images were resized to 768 x 768 pixels and the vessels were located, then the AF images were registered to the IR images using the method described in IIIB. All the images in this data set were well-registered with this method, but we recognize that there may be shortcomings with this approach in the future. The neural network classifier was implemented using the MATLAB programming environment neural network toolbox for the supervised learning algorithm. Images were processed on a hold-one-out basis per image; each image was held-out, a neural network was created and trained, and then the held-out image was classified on a pixel-by-pixel basis. The neural network was configured with two layers of 20 nodes each and used the Scaled Conjugate Gradient learning algorithm with the mean-square-error as the objective function. The images were processed at quarter-size to improve speed of processing.

### C. Results

The approach performed reasonably well, achieving a sensitivity of 82.5% and specificity of 92.9% as measured on a per-pixel basis and averaged across all the input image pairs. The training time was somewhat slow, requiring approximately an hour per image on a 64 bit PC with a 3.16 GHz processor and 4 GBytes of RAM. Some examples of segmentation are shown in Figure 3 and Figure 4.

## V. CONCLUSION

In this work we used two imaging modalities, IR and AF images, to perform automated segmentation of geographic atrophy. The algorithm performed well on this data set and is a promising start for this area of medical imaging research. In future work, we would like to extend our analysis to additional post-processing steps to more completely delineate the disease boundary. We also hope to expand our analysis with additional features as more data is acquired (possibly using parallel processing implementations to reduce computational time), and use additional quantitative measures for comparison with ground truth besides pixel-based sensitivity and specificity. Finally, there are other regions of interest in AMD images (including drusen and exudates) which could benefit from a similar segmentation approach. Finally, we would like to conduct a comparison study of this supervised learning method with other segmentation methods (such as active contours and level-sets).

## REFERENCES


[1] Abramoff, M.D., Niemeijer, M., and Russell, S.R., (2010) Automated detection of diabetic retinopathy: barriers to translation into clinical practice, Expert Rev. Medical Devices 7:287-296

[2] Sarks. Aging and degeneration in the macular region. A clinical-pathological study. Br J Ophthalmol1976;60(5): 324-41

[3] Sarks JP, Sarks SH, Killingsworth MC. Evolution of geographic atrophy of the retinal pigment epithelium. Eye.1988;2(5):552--7

[4] Tobin KW, Chaum E, Govindasamy VP, Karnowski TP. (2007) Detection of anatomic structures in human retinal imagery. IEEE Trans Med Imaging 26:1729-39

[5] Zana, F., Klein, J., (2001) Segmentation of vessel-like patterns using mathematical morphology and curvature evaluation. IEEE Trans. Image Processing, 10:1010-1019

[6] Can, A., Stewart, C.V., Roysam, B.: Robust hierarchical algorithm for constructing a mosaic from images of the curved human retina. In: IEEE Conference on Computer Vision and Pattern Recognition. Volume 2. (1999) 286–92

[7] Hart, W.E., Goldbaum, M.H.: Registering retinal images using automatically selected control point pairs. In: Proc. IEEE International Conference on Image Processing (ICIP). Volume 3. (1994) 576–81

[8] Becker, D.E., Can, A., Turner, J.N., Tanenbaum, H.L., Roysam, B.: Image processing algorithms for retinal montage synthesis, mapping, and real-time location determination. IEEE Trans. on Biomedical Engineering 45 (1998) 105–18

[9] Dickey, F.M. and Romero, L.A., (1991), "Normalized correlation for pattern recognition", Optics Letters, v. 16 pp 1186-1188

[10] J.J. Staal, M.D. Abramoff, M. Niemeijer, M.A. Viergever, B. van Ginneken, "Ridge based vessel segmentation in color images of the retina", IEEE Transactions on Medical Imaging, 2004, vol. 23, pp. 501-509.